Int. J. Heat Mass Transfer. Vol. 31, No. 6, pp. 1149–1156, 1988
Printed in Great Britain

0017-9310/88 $3.00+0.00
Pergamon Press plc

Non-stationary conjugate free-convective heat transfer in horizontal cylindrical coaxial channels

P. M. KOLESNIKOV and V. I. BUBNOVICH
Luikov Heat and Mass Transfer Institute, 220728, Minsk, U.S.S.R.

(*Received* 18 *June* 1985)

Abstract—A conjugate problem of natural convection in a horizontal annulus is solved numerically; a comparison of the solution with non-conjugate problems is given; the effect of walls on heat transfer in a channel is shown.

1. INTRODUCTION

THE STUDY of heat transfer in coaxial cylindrical channels is of great importance for calculation of different heat exchangers, apparatus for chemical engineering technology, plasmatrons, plasma accelerators, radio-electronic devices, cryogenic power transmission lines, solar energy converters, etc.

The processes of heat and mass transfer by laminar free convection between horizontal isothermal concentric cylinders were studied theoretically [1, 2], by numerical methods [3, 4] and experimentally [5, 6]. In the overwhelming majority of the above-mentioned papers stationary solutions of the problem are suggested; non-stationary problems were the concern of refs. [7, 8]. Turbulent free convection in a gap between horizontal concentric cylinders was considered in ref. [4]. A very detailed review of the literature on natural convection in an annulus under various thermal boundary conditions is given in refs. [7, 9–11].

A conjugate formulation of the problem of free convection in annuli was studied to a lesser extent in refs. [11–13]. In ref. [13] a stationary conjugate problem of natural convection in a gap between a coaxial hollow cylinder and a cylindrical rod is treated by asymptotic methods. The mathematical simulation of three- and two-dimensional conjugate problems of natural convection and corresponding conjugation criteria were the concern of refs. [14–16].

This paper considers the unsteady-state conjugate heat transfer by natural convection between horizontal coaxial hollow cylinders, comparison is drawn between similar problems in non-conjugate formulation, a considerable influence of walls on heat transfer in channels is shown.

2. BASIC EQUATIONS AND PARAMETERS OF THE PROBLEM

Making use of the cylindrical system of coordinates, assume that the angular coordinate ϕ is measured from the vertical directed downwards ($\phi = 0$) and the problem is symmetric about a vertical plane passing through the axis of the cylinders [5], therefore, consideration will be confined to the range $0 \leqslant \phi \leqslant \pi$ (Fig. 1).

Assuming the thermophysical properties of an incompressible fluid to be constant, consider non-stationary convection in the space limited by two coaxial cylindrical tubes.

Equations of heat and mass transfer in the fluid and tube walls have the form:

continuity equation

$$\frac{1}{r}\frac{\partial}{\partial r}(rv_r)+\frac{1}{r}\frac{\partial v_\phi}{\partial \phi}=0; \tag{1}$$

motion equations

$$\frac{\partial v_r}{\partial t}+v_r\frac{\partial v_r}{\partial r}+\frac{v_\phi}{r}\frac{\partial v_r}{\partial \phi}-\frac{v_\phi^2}{r}=-\frac{1}{\rho}\frac{\partial P}{\partial r}+\nu\left[\frac{\partial}{\partial r}\left(\frac{1}{r}\frac{\partial}{\partial r}(rv_r)\right)+\frac{1}{r^2}\frac{\partial^2 v_r}{\partial \phi^2}-\frac{2}{r^2}\frac{\partial v_\phi}{\partial \phi}\right]+g[1-\beta(T-T_o)]\cos\phi \tag{2}$$

$$\frac{\partial v_\phi}{\partial t}+v_r\frac{\partial v_\phi}{\partial r}+\frac{v_\phi}{r}\frac{\partial v_\phi}{\partial \phi}+\frac{v_r v_\phi}{r}=-\frac{1}{r\rho}\frac{\partial P}{\partial \phi}+\nu\left[\frac{\partial}{\partial r}\left(\frac{1}{r}\frac{\partial}{\partial r}(rv_\phi)\right)+\frac{1}{r^2}\frac{\partial^2 v_\phi}{\partial \phi^2}+\frac{2}{r^2}\frac{\partial v_r}{\partial \phi}\right]-g[1-\beta(T-T_o)]\sin\phi; \tag{3}$$

equation of energy in the fluid

$$\frac{\partial T_2}{\partial t}+v_r\frac{\partial T_2}{\partial r}+\frac{v_\phi}{r}\frac{\partial T_2}{\partial \phi}=a_2\left[\frac{1}{r}\frac{\partial}{\partial r}\left(r\frac{\partial T_2}{\partial r}\right)+\frac{1}{r^2}\frac{\partial^2 T_2}{\partial \phi^2}\right]; \tag{4}$$

equation of thermal transfer in the walls

$$\frac{\partial T_1}{\partial t}=a_1\left[\frac{1}{r}\frac{\partial}{\partial r}\left(r\frac{\partial T_1}{\partial r}\right)+\frac{1}{r^2}\frac{\partial^2 T_1}{\partial \phi^2}\right]. \tag{5}$$

NOMENCLATURE

a	thermal diffusivity
$\tilde{a}$	ratio of thermal diffusivities, a_1/a_2
b'	inner cylinder wall thickness
b	dimensionless wall thickness of inner cylinder
c'	outer cylinder wall thickness
c	dimensionless wall thickness of outer cylinder
Fo	Fourier number, $a_2 t/r_i^2$
g	gravity acceleration
Gr_i	Grashof number, $\beta g(T_i - T_o)r_i^3/\nu^2$
Gr_o	$\beta g(T_i - T_o)r_o^3/\nu^2$
Gr	$\beta g(T_i - T_o)(r_o - r_i)^3/\nu^2$
h	step of a spatial grid $(\Delta R, \Delta\phi)$
Nu	Nusselt number
$\overline{Nu}$	mean Nusselt number
Pr	Prandtl number
P	fluid pressure
Ra	Rayleigh number, $Gr\,Pr$
R	dimensionless radial coordinate
r	radial coordinate
t	time
T	temperature
u	dimensionless radial velocity component, $v_r r_i/a_2$
v_r	radial velocity component
v_ϕ	angular velocity component
v	dimensionless angular velocity component, $v_\phi r_i/a_2$.

Greek symbols

β	coefficient of thermal expansion of fluid
η	ratio of radii, r_o/r_i
θ	dimensionless temperature, $(T-T_o)/(T_i-T_o)$
λ	thermal conductivity
$\tilde{\lambda}$	thermal conductivity ratio, λ_2/λ_1
ν	coefficient of kinematic viscosity
ρ	fluid density
τ	relaxation parameter
ϕ	polar coordinate
Ψ	stream function
ψ	dimensionless stream function, Ψ/a_2
Ω	vorticity
ω	dimensionless vorticity, $\Omega r_i^2/a_2$.

Subscripts

i	inner cylinder
o	outer cylinder
1	wall
2	fluid
k, j	spatial indices of grid nodes
n	number of time layer.

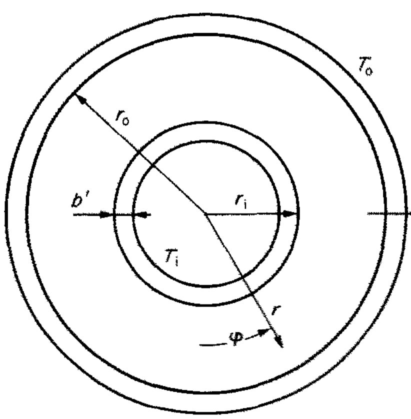

FIG. 1. Channel geometry.

The initial conditions will be assumed as follows:

$$v_r = v_\phi = 0, \quad T_1 = T_2 = T_o \quad \text{at } t = 0. \tag{6}$$

The boundary conditions at the fluid–wall interface are:

no-slip condition

$$v_r = v_\phi = 0 \quad \text{at } r = r_i \text{ and } r = r_o; \tag{7}$$

conjugation condition

$$\lambda_1 \frac{\partial T_1}{\partial r} = \lambda_2 \frac{\partial T_2}{\partial r}, \quad T_1 = T_2 \quad \text{at } r = r_i \text{ and } r = r_o. \tag{8}$$

It is assumed on the line of symmetry that

$$v_\phi = \frac{\partial v_r}{\partial \phi} = \frac{\partial T_1}{\partial \phi} = \frac{\partial T_2}{\partial \phi} = 0.$$

On the outer boundaries of the walls the boundary conditions of the first kind are prescribed

$$T_1 = T_i \quad \text{at } r = r_i - b' \quad \text{and} \quad T_1 = T_o \quad \text{at } r = r_o + c' \tag{9}$$

with $T_i > T_o$.

On the introduction of the stream function Ψ, defined by the relations

$$v_\phi = \frac{\partial \Psi}{\partial r}, \quad v_r = -\frac{1}{r}\frac{\partial \Psi}{\partial \phi} \tag{10}$$

continuity equation (1) is satisfied identically.

Multiplying equation (3) by r, then performing the operations $(1/r)(\partial/\partial\phi)$ and $(\partial/\partial r)$ on equations (2) and (3), respectively, and substracting one equation from the other, it is possible to eliminate the pressure variable. Then the basic equations for the dimensionless stream function, velocity and temperatures will take the form

$$\omega = -\nabla^2\psi \tag{11}$$

$$\frac{\partial\omega}{\partial Fo}+u\frac{\partial\omega}{\partial R}+\frac{v}{R}\frac{\partial\omega}{\partial\phi} = Pr\nabla^2\omega + Gr\,Pr^2\left[\sin\phi\frac{\partial\theta_2}{\partial R}+\frac{\cos\phi}{R}\frac{\partial\theta_2}{\partial\phi}\right] \tag{12}$$

$$\frac{\partial\theta_2}{\partial Fo}+u\frac{\partial\theta_2}{\partial R}+\frac{v}{R}\frac{\partial\theta_2}{\partial\phi} = \nabla^2\theta_2 \tag{13}$$

$$\frac{\partial\theta_1}{\partial Fo} = \tilde{a}\nabla^2\theta_1 \tag{14}$$

where the dimensionless quantities are introduced

$$R = r/r_i, \quad \omega = \Omega r_i^2/a_2,$$
$$\psi = \Psi/a_2, \quad \theta = (T-T_o)/(T_i-T_o),$$
$$Fo = a_2 t/r_i^2, \quad u = v_r r_i/a_2,$$
$$v = v_\phi r_i/a_2, \quad \tilde{a} = a_1/a_2. \tag{15}$$

The initial and boundary conditions are written here as

$$\psi = \omega = \theta_1 = \theta_2 = 0 \quad \text{at } Fo = 0 \tag{16}$$

$$\psi = \omega = \frac{\partial\theta_1}{\partial\phi} = \frac{\partial\theta_2}{\partial\phi} = 0 \quad \text{along } \phi = 0, \pi \text{ (symmetry line)} \tag{17}$$

$$\left.\begin{array}{l} \theta_1 = \theta_2, \quad \tilde{\lambda}\dfrac{\partial\theta_2}{\partial R} = \dfrac{\partial\theta_1}{\partial R} \\ \psi = \partial\psi/\partial R = 0 \quad \text{at } R = 1 \\ \theta_1 = 1 \quad \text{at } R = 1-b \end{array}\right\} \text{(inner cylinder)} \tag{18}$$

$$\left.\begin{array}{l} \theta_1 = \theta_2, \quad \tilde{\lambda}\dfrac{\partial\theta_2}{\partial R} = \dfrac{\partial\theta_1}{\partial R} \\ \psi = \partial\psi/\partial R = 0 \quad \text{at } R = \eta \\ \theta_1 = 0 \quad \text{at } R = \eta + c \end{array}\right\} \text{(outer cylinder).} \tag{19}$$

The boundary condition for vorticity on the walls will be taken in the form [9, 17]

$$\omega = -\frac{\partial^2\psi}{\partial R^2}, \quad R = 1, \eta. \tag{20}$$

The set of equations (11)–(14) and boundary conditions (16)–(20) incorporate the following dimensionless parameters:

(1) the Prandtl number $Pr = \nu/a_2$;

(2) the Grashof number $Gr_i = g\beta(T_i - T_o)r_i^3/\nu^2$;

(3) the ratio between the thermal conductivities of the fluid and the wall under the conjugation conditions $\tilde{\lambda} = \lambda_2/\lambda_1$;

(4) the ratio between the thermal conductivities of the fluid and the wall in equation (14) $\tilde{a} = a_1/a_2$;

(5) the outer to the inner radius ratio (r_o/r_i) which characterizes the size of the gap in the channel $\eta = r_o/r_i$;

(6) the relative thickness of the channel walls $b = b'/r_i$, $c = c'/r_i$.

3. ALGORITHM FOR THE CONJUGATE PROBLEM SOLUTION

The system of equations (11)–(14) with initial condition (16) and boundary conditions (17)–(20) was solved numerically by the alternating-direction method using the implicit finite-difference scheme [17]. The space grid was selected to be uniform ($\Delta\phi = \pi/20$) in the direction of ϕ, while in the r-direction it was divided into three regions with different constant steps. The mesh steps were taken smaller near the wall than in the centre of the annulus.

The convective terms were approximated by non-symmetric difference relations with the so-called 'opposite-to-flow orientation' [17].

At the boundaries of the region, the first- and second-order partial derivatives were determined, when making the approximation towards the centre region, from the following relations:

$$\frac{\partial f}{\partial n} = \frac{-3f_o+4f_1-f_2}{2h}+O(h^2) \tag{21}$$

$$\frac{\partial^2 f}{\partial n^2} = \frac{-7f_o+8f_1-f_2}{2h^2}-\frac{3}{h}\left(\frac{\partial f}{\partial n}\right)\bigg|_0+O(h^2) \tag{22}$$

where

$$n = (\phi, R), \quad f = (u, \psi, \theta_1, \theta_2).$$

The conditions for the conjugation of the temperatures on the inner and outer cylinders were transformed, respectively, into the difference equations

$$\theta^n_{1kj} = \theta^n_{2kj}, \quad \frac{\theta^n_{1kj}-\theta^n_{1kj-1}}{\Delta R_{j-1}} = \tilde{\lambda}\frac{\theta^n_{2kj+1}-\theta^n_{2kj}}{\Delta R_j} \quad \text{at } R = 1$$

$$\theta^n_{2kj} = \theta^n_{1kj}, \quad \tilde{\lambda}\frac{\theta^n_{2kj}-\theta^n_{2kj-1}}{\Delta R_{j-1}} = \frac{\theta^n_{1kj+1}-\theta^n_{1kj}}{\Delta R_j} \quad \text{at } R = \eta. \tag{23}$$

The elliptic equation (11) was solved by the time-dependent technique and therefore the relaxation parameter τ was introduced

$$\tau = \min\begin{Bmatrix}\Delta R_j \\ \Delta\phi\end{Bmatrix} \tag{24}$$

and equation (11) became parabolic. It was solved by the alternating-direction method [17]; the factorized terms in the directions R and ϕ were closed by equations (21) and (22), respectively. Iterations on any time step stop after the following convergence criterion is satisfied:

$$\sum \left| \overset{s+1}{\psi}{}^{n}_{kj} - \overset{s}{\psi}{}^{n}_{kj} \right| \Big/ \sum \left| \overset{s+1}{\psi}{}^{n}_{kj} \right| < 10^{-3}. \quad (25)$$

The number of iterations decreased rapidly from 25 to 30 at the initial instants of time to 2–4 with the steady-state regime being approached. Depending on the numbers Pr, Gr and η, each interval of time steps constitutes from 200 to 300. During the successive solution of equations (11) and (12) the residual in the boundary nodes was eliminated following the numerical scheme in ref. [18]. At the prescribed Gr, Pr, η, $\tilde{\lambda}$, $\tilde{a}$, b, c and initial distributions of θ_1, θ_2, ψ, ω, u and v, calculations on one time step incorporate the following operations: first, equations (11)–(14) are solved successively by the above-mentioned method; then from equations (10) the velocity field is found in terms of central differences, and from [3, 10]

$$Nu_i = \ln(\eta) \left[\frac{\partial \theta_2}{\partial R}\right]\Bigg|_{R=1},$$

$$Nu_o = -\eta \ln(\eta) \left[\frac{\partial \theta_2}{\partial R}\right]\Bigg|_{R=\eta} \quad (26)$$

the local Nusselt numbers are determined for the surfaces of the inner and outer cylinders, respectively, and, finally, with the aid of the expressions

$$\overline{Nu}_i = \frac{1}{\pi}\int_0^{\pi} Nu_i \, d\phi, \quad \overline{Nu}_o = \frac{1}{\pi}\int_0^{\pi} Nu_o \, d\phi \quad (27)$$

mean Nusselt numbers are calculated for each cylinder. The integrals indicated were found numerically using the Simpson rule. The total Nusselt number $\overline{Nu}$ was determined as the arithmetic mean of $\overline{Nu}_i$ and $\overline{Nu}_o$.

The transitions from the solution of the conjugate to a non-conjugate problem in the method considered was made by the limiting transition

$$\tilde{\lambda} \to 0.$$

Moreover, a separate programme was used for solving non-conjugate problems to check the computation.

4. BASIC RESULTS. COMPARISON BETWEEN CONJUGATE AND NON-CONJUGATE PROBLEMS

In order to reveal the effect of channel walls on heat transfer and to compare the solutions of conjugate and non-conjugate problems and also to verify the reliability of a numerical algorithm, calculations were made for the following variants convenient for comparison with earlier works [1, 3, 10]: (1) $Pr = 0.02$, $\eta = 5$, $Gr_o = 200$; (2) $Pr = 0.7$, $\eta = 1.57$, $Ra_i = 14\,420$; (3) $Pr = 0.7$: (a) $\eta = 1.5$, $Gr = 4850$;

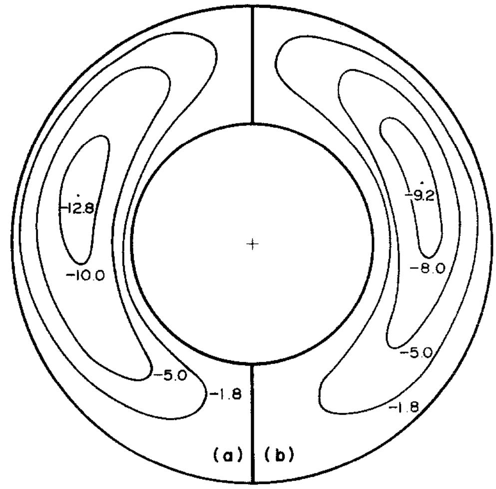

FIG. 2. Stream lines for the non-conjugate (a) and conjugate (b) problems, respectively.

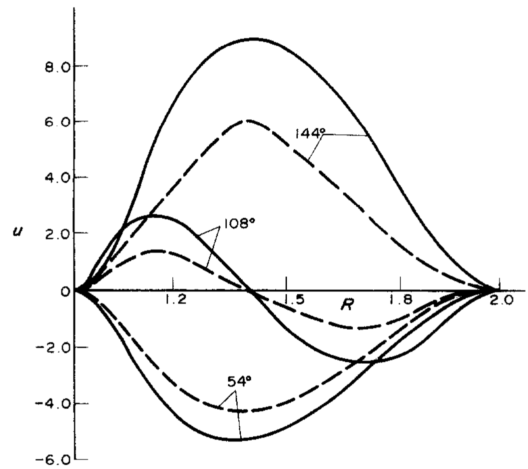

FIG. 3. Radial velocity component: — — —, conjugate problem; ———, non-conjugate problem.

(b) $\eta = 2$, $Gr = 10\,000$; (c) $\eta = 2$, $Gr = 26\,600$; (d) $\eta = 2$, $Gr = 38\,800$.

For the above parameters equations (11)–(14) were solved in both conjugate and non-conjugate formulations. The analysis of the results showed that with $\tilde{\lambda} \to 0$ these solutions coincided. Moreover, the temperature profiles, just as the flow structure, which were found from the solutions obtained, turned to be identical in character with the results of refs. [1, 3, 10]. The greatest discrepancy was found when comparing with the solution obtained in ref. [3], for local Nusselt numbers near the regions $\phi = 0°$ and $180°$, it did not exceed 12%. This difference is due to the fact that at Grashof numbers close to transient ones, condition (25) does not furnish the estimation of the real error when solving the Poisson equation. Thus, a conjugate problem was solved with the parameters: $Pr = 0.7$, $Gr_i = 10\,000$, $\eta = 2$, $\tilde{a} = 2.0$, $\tilde{\lambda} = 0.4$, $b = c = 0.2$. The data on hydrodynamics (Figs. 2–4) and heat transfer (Figs. 5–9) resulting from the solution of this problem, were then compared with the corresponding solution

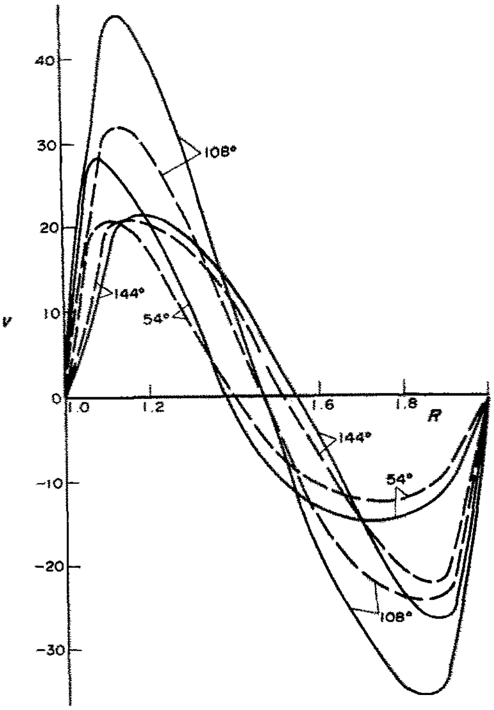

FIG. 4. Angular velocity component: ———, conjugate problem; ———, non-conjugate problem.

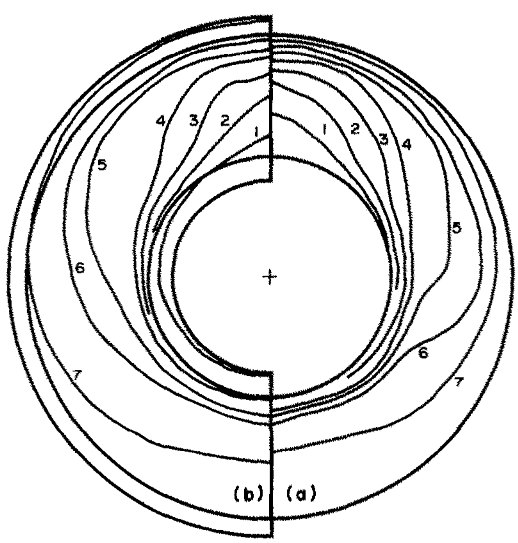

FIG. 5. Predicted isotherms for the non-conjugate (a) and conjugate (b) problems, respectively: 1, $\theta = 0.9$; 2, 0.8; 3, 0.7; 4, 0.6; 5, 0.4; 6, 0.3; 7, 0.1.

of this very problem in a non-conjugate formulation. Below, an analysis and comparison are made of the problem solution in conjugate and non-conjugate formulations.

The measure of the motion intensity of an incompressible fluid is provided by the maximum absolute value of the stream function, with other conditions remaining constant. Making use of this criterion it can be seen from Fig. 2 that the fluid motion intensity found from the non-conjugate problem solution

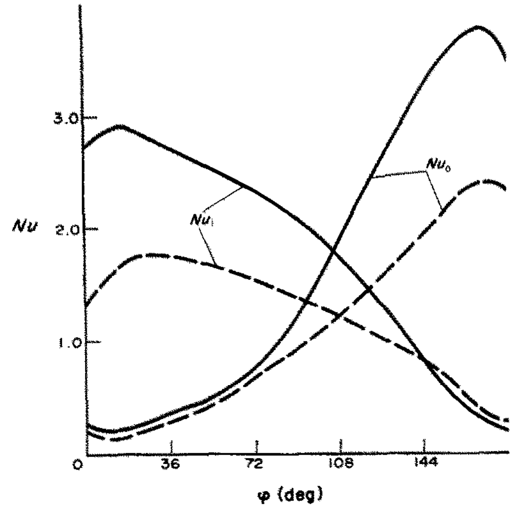

FIG. 6. Local Nusselt numbers: ———, conjugate problem; ———, non-conjugate problem.

exceeds the analogous characteristics of the conjugate problem by a factor of 1.39. In this case the vortex centre in the conjugate problem shifted upwards by $\Delta\phi \approx 6°$ with respect to the vortex centre in the non-conjugate problem. Figures 3 and 4 contain comparison between the radial and angular velocity components in the sections $\phi = 54°$, $108°$ and $154°$. It is seen from the figure that allowing for the thermal conductivity of the channel walls reduces the angular and radial velocities of the fluid non-uniformly over the entire channel. Thus, in the fluid layer adjacent to the inner cylinder the greatest differences in the velocity v are observed in the lower portion of the annulus ($0° \leqslant \phi \leqslant 140°$), and conversely, in the fluid layer at the opposite wall—in the upper portion of the channel ($75° \leqslant \phi \leqslant 180°$).

A comparison of the heat transfer data is given in Figs. 5–9. The transference of thermal boundary conditions from the inner to the outer surfaces of the channel walls in the conjugate problem led to the redistribution of isotherms in the channel (Fig. 5) and, naturally, to a change in the distribution of local Nusselt numbers on both walls (Fig. 6). On the inner cylinder (Fig. 6), within the range $140° \leqslant \phi \leqslant 180°$, the local Nusselt numbers Nu_i for the conjugate and non-conjugate problems nearly coincide and differ insignificantly; with a decrease of ϕ from 140° to 0° the difference between them progressively increases and at $\phi = 0°$ they differ by 70%. The reverse is true for the case on the outer cylinder: over the portion $0° \leqslant \phi \leqslant 75°$ they differ slightly, whereas with an increase of ϕ from 75° to 180° the disagreement becomes increasingly pronounced. In Figs. 7(a) and (b) the temperature distributions along the radii are presented for the non-conjugate and conjugate problems, respectively. These graphs show that the course of the temperature curves and their slope to the axes R and θ differ greatly for both problems within the ranges $1 \leqslant R \leqslant 1.2$ and $1.8 \leqslant R \leqslant 2.0$. Moreover, the

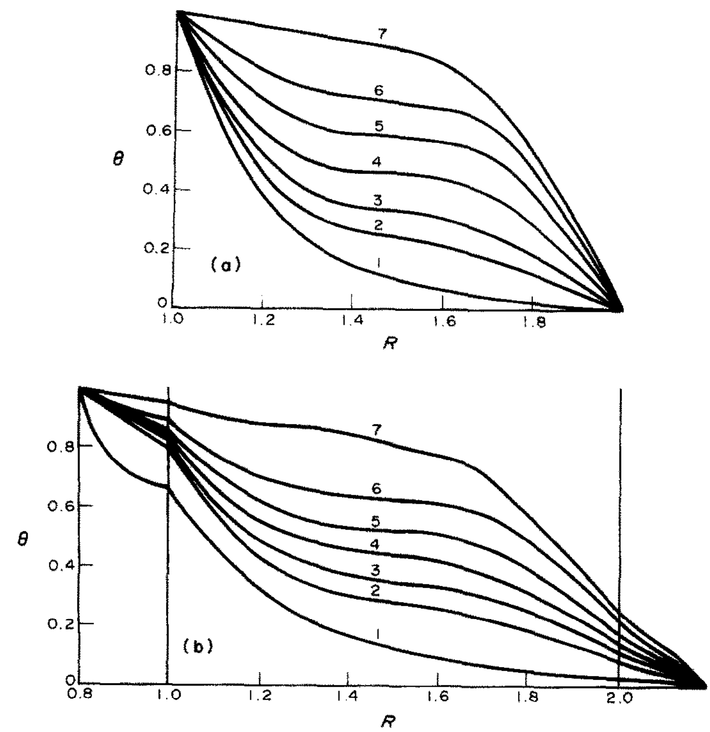

FIG. 7. Temperature distribution along a radius for the non-conjugate (a) and conjugate (b) problems, respectively: 1, 0°; 2, 72°; 3, 90°; 4, 108°; 5, 126°; 6, 144°; 7, 180°.

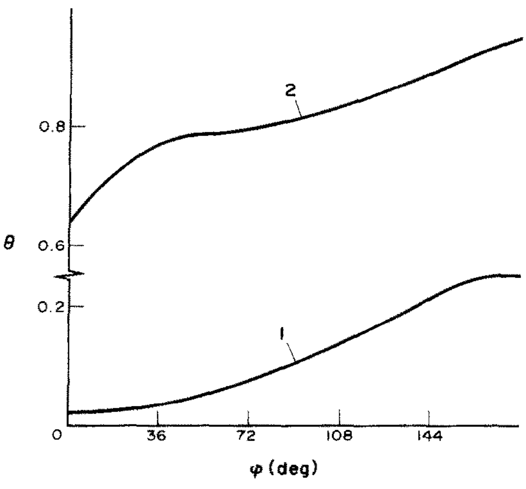

FIG. 8. Temperature distribution over the interfaces between the walls and the fluid for inner (1) and outer (2) cylinders, respectively.

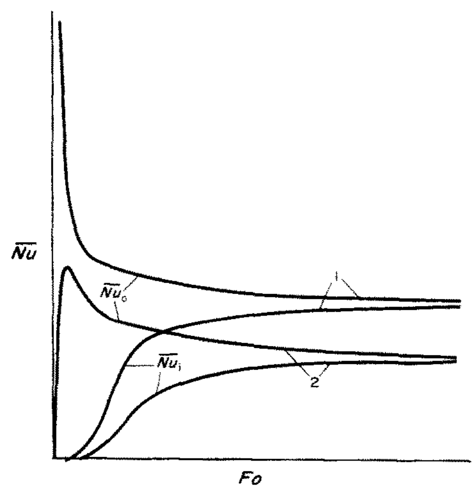

FIG. 9. Time dependence of the mean numbers $\overline{Nu}_i$ and $\overline{Nu}_o$ for the non-conjugate (1) and conjugate (2) problems, respectively.

flattened portions of the curves $\phi = 126°$, $144°$ and $180°$ of the non-conjugate problem are located above the analogous curves of the conjugate problem, while for the curves $\phi = 90°$, $72°$ and $0°$ the reverse phenomenon is observed. Figure 8 illustrates the distribution of the temperature θ, found from the conjugate problem solution, along the interface surface between the fluid and the inner and outer cylinders. It is seen that while within the range $35° \leqslant \phi \leqslant 160°$ both curves have nearly the same angles of inclination to the axes ϕ and θ, then near the regions $\phi = 0°$ and $180°$ these angles differ greatly.

Figure 9 shows the time history of mean Nusselt numbers on both channel walls. The data on the steady-state heat transfer regimes makes it possible to assert that allowance for the finite thickness of the channel walls and conjugation of temperature fields at the fluid–wall interface led to a decrease of $\overline{Nu}$ by a factor of 1.42. Moreover, the curve $\overline{Nu}_o(Fo)$ for the conjugate problem in contrast to the non-conjugate one has a maximum point and tends to zero as $Fo \to 0$.

5. CONCLUSIONS

The problem of conjugate unsteady-state natural convection in a gap between horizontal coaxial cylindrical tubes is solved using an implicit scheme by a numerical method based on the factorization for ω, ψ and θ successively along the radius R and then over the angle ϕ. The numerical solution makes it possible to analyse in detail the patterns of stream lines and isotherms in the fluid and also the course of isotherms in channel walls. The applied numerical method can be extended to the problems of unsteady-state free convection with different thermal boundary conditions on the channel walls with different geometrical relationships.

The above calculations show that taking into account the channel wall greatly affects the natural convection heat transfer.

The study of the influence of such parameters as $\tilde{\lambda}$, $\tilde{a}$, b and c on the solution of the conjugate problem of natural convection in an annulus was made earlier in ref. [19].

REFERENCES

1. J. R. Custer and E. J. Shaughnessy, Thermoconvective motion of low Prandtl number fluids within a horizontal cylindrical annulus, *Trans. ASME, J. Heat Transfer* **99**(4), 97–105 (1977).
2. L. R. Mack and E. H. Bishop, Natural convection between horizontal concentric cylinders for low Rayleigh numbers, *Q. J. Mech. Appl. Math.* **21**(2), 223–241 (1968).
3. R. E. Powe, C. T. Carley and C. L. Carruth, A numerical solution for natural convection in cylindrical annuli, *Trans. ASME, J. Heat Transfer* **93**(2), 78–87 (1971).
4. B. Farouk and S. I. Guceri, Laminar and turbulent natural convection in the annulus between horizontal concentric cylinders, *Trans. ASME, J. Heat Transfer* **104**(4), 55–59 (1982).
5. R. E. Powe, C. T. Carley and E. H. Bishop, Free convective flow patterns in cylindrical annuli, *Trans. ASME, J. Heat Transfer* **91**(3), 18–24 (1969).
6. T. H. Kuehn and R. J. Goldstein, An experimental and theoretical study of natural convection in the annulus between horizontal concentric cylinders, *J. Fluid Mech.* **74**, 695–719 (1976).
7. L. C. Charrier-Mojtabi, A. Mojtabi and J. P. Caltagirone, Numerical solution of a flow due to natural convection in horizontal cylindrical annuli, *Trans. ASME, J. Heat Transfer* **101**(1), 199–201 (1979).
8. B. E. Vasilik, B. B. Petrazhitsky, M. A. Rozanov and L. N. Shukin, Numerical study of the initial stage of the convective heat transfer process development in a horizontal annular cavity, *Coll. Pap. Moscow Pwr Engng Inst.* No. 588, 24–30 (1982).
9. T. H. Kuehn and R. J. Goldstein, A parametric study of Prandtl number and diameter ratio effects on natural convection heat transfer in horizontal cylindrical annuli, *Trans. ASME, J. Heat Transfer* **102**(4), 196–198 (1980).
10. Y. T. Tsui and B. Tremblay, On transient natural convection heat transfer in the annulus between concentric, horizontal cylinders with isothermal surfaces, *Int. J. Heat Mass Transfer* **27**(1), 103–111 (1984).
11. V. I. Bubnovich and P. M. Kolesnikov, Transient conjugate natural convection heat transfer in horizontal cylindrical coaxial channels. In *Mathematical Models of the Theory of Transfer in Inhomogeneous and Non-linear Media with Phase Transition*, pp. 25–45. ITMO AN BSSR, Minsk (1986).
12. V. I. Bubnovich, Numerical study of natural convection in cylindrical coaxial channels. In *Heat Mass Transfer and Physicochemical Processes in Power Plants*, pp. 40–45. ITMO AN BSSR, Minsk (1985).
13. Zeev Rotem, Conjugate free convection from horizontal, conducting circular cylinders, *Int. J. Heat Mass Transfer* **15**, 1679–1693 (1972).
14. V. S. Kuptsova, Conjugation criteria in the problems of free-convective heat transfer, *Vestsi AN BSSR, Ser. Fiz.-Energ. Navuk* No. 4, 93–104 (1985).
15. V. S. Kuptsova, Numerical study of thermal and concentrational convection under the conditions of conjugate heat transfer. In *Problems of Viscous Flows*, pp. 117–131. *Proc. 8th All-Union School-Seminar on Numerical Methods of the Mechanics of Viscous Fluids*, Novosibirsk (1981).
16. V. S. Kuptsova, Mathematical models of conjugate problems of natural convection, *Vestsi AN BSSR, Ser. Fiz.-Energ. Navuk* No. 3, 52–58 (1985).
17. V. M. Paskonov, V. I. Poleshaev and L. A. Chudov, *Numerical Simulation of Heat and Mass Transfer Processes*. Izd. Nauka, Moscow (1984).
18. A. G. Daikovsky, V. I. Poleshaev and L. I. Fedoseyev, On calculation of boundary conditions for the non-stationary Navier–Stokes equations in the variables vortex, stream function, *Chisl. Metody Mekh. Sploshn. Sredy* **10**(2), 61–66 (1979).
19. V. I. Bubnovich and P. M. Kolesnikov, Conjugate unsteady-state heat transfer during laminar natural convection in a horizontal annulus, *J. Engng Phys.* **51**(4), 576–583 (1986).

TRANSFERT THERMIQUE CONJUGUE DE CONVECTION LIBRE VARIABLE DANS DES ESPACES ANNULAIRES HORIZONTAUX

Résumé—On résout un problème conjugué de convection naturelle dans un espace annulaire horizontal. Une comparaison avec la solution du problème non conjugué est donnée. On montre les effets de paroi sur le transfert thermique.

INSTATIONÄRER KONJUGIERTER WÄRMEÜBERGANG DURCH FREIE KONVEKTION IN WAAGERECHTEN KOAXIALEN ZYLINDRISCHEN KANÄLEN

Zusammenfassung—Ein konjugiertes Problem der natürlichen Konvektion in einem waagerechten Ringraum wird numerisch untersucht. Die Lösung wird mit derjenigen für den nicht-konjugierten Fall verglichen. Der Wandeffekt auf den Wärmeübergang in einem Kanal wird gezeigt.

НЕСТАЦИОНАРНЫЙ СОПРЯЖЕННЫЙ ТЕПЛОПЕРЕНОС ЕСТЕСТВЕННОЙ КОНВЕКЦИЕЙ В ГОРИЗОНТАЛЬНЫХ ЦИЛИНДРИЧЕСКИХ КОАКСИАЛЬНЫХ КАНАЛАХ

Аннотация—Численно решена сопряженная задача естественной конвекции в горизонтальном кольцевом зазоре, приведны сопоставления решений с несопряженными задачами, показано влияние стенок на теплоотдачу в канале.